

## ORIGINAL ARTICLE

# Selective targeting of IRF4 by synthetic microRNA-125b-5p mimics induces anti-multiple myeloma activity *in vitro* and *in vivo*

E Morelli<sup>1</sup>, E Leone<sup>1</sup>, ME Gallo Cantafio<sup>1</sup>, MT Di Martino<sup>1</sup>, N Amodio<sup>1</sup>, L Biamonte<sup>1</sup>, A Gullà<sup>1</sup>, U Foresta<sup>1</sup>, MR Pitari<sup>1</sup>, C Botta<sup>1</sup>, M Rossi<sup>1</sup>, A Neri<sup>2</sup>, NC Munshi<sup>3,4</sup>, KC Anderson<sup>3</sup>, P Tagliaferri<sup>1</sup> and P Tassone<sup>1,5</sup>

Interferon regulatory factor 4 (IRF4) is an attractive therapeutic target in multiple myeloma (MM). We here report that expression of IRF4 mRNA inversely correlates with microRNA (miR)-125b in MM patients. Moreover, we provide evidence that miR-125b is downregulated in TC2/3 molecular MM subgroups and in established cell lines. Importantly, constitutive expression of miR-125b-5p by lentiviral vectors or transfection with synthetic mimics impaired growth and survival of MM cells and overcame the protective role of bone marrow stromal cells *in vitro*. Apoptotic and autophagy-associated cell death were triggered in MM cells on miR-125b-5p ectopic expression. Importantly, we found that the anti-MM activity of miR-125b-5p was mediated via direct downregulation of IRF4 and its downstream effector BLIMP-1. Moreover, inhibition of IRF4 translated into downregulation of c-Myc, caspase-10 and cFlip, relevant IRF4-downstream effectors. Finally, *in vivo* intra-tumor or systemic delivery of formulated miR-125b-5p mimics against human MM xenografts in severe combined immunodeficient/non-obese diabetic mice induced significant anti-tumor activity and prolonged survival. Taken together, our findings provide evidence that miR-125b, differently from other hematologic malignancies, has tumor-suppressor activity in MM. Furthermore, our data provide proof-of-concept that synthetic miR-125b-5p mimics are promising anti-MM agents to be validated in early clinical trials.

Leukemia (2015) 29, 2173–2183; doi:10.1038/leu.2015.124

## INTRODUCTION

Multiple myeloma (MM) is a genetically complex malignancy from the outset, with progressive acquisition of genetic lesions mediating drug resistance and high disease burden.<sup>1</sup> Despite recent progress in the understanding MM pathobiology and the availability of innovative drugs which have improved clinical outcome, the disease eventually progresses to a drug-resistant lethal stage (plasma cell leukemia)<sup>2–4</sup> and novel therapeutic strategies are therefore eagerly awaited. Indeed, one of the major challenges in treating MM is its genomic and phenotypic heterogeneity.<sup>5</sup> Hence, an optimal therapy would target an essential regulatory pathway shared by all disease subsets.<sup>6</sup>

Interferon regulatory factor 4 (IRF4) is a lymphocyte-specific transcription factor.<sup>7</sup> Interference with IRF4 expression is lethal for MM cells, irrespective of their genetics, making IRF4 an ‘Achilles’ heel’ that may be exploited therapeutically.<sup>8</sup> Specifically, IRF4 is oncogenic and overexpressed when translocated to actively transcribed genomic regions in some MM patients, but it also has a survival effect in MM cells in the absence of translocations or overexpression.<sup>7,8</sup> A relevant IRF4 target gene is c-Myc,<sup>7,8</sup> which has a prominent role in the pathogenesis of MM.<sup>7,8</sup> Another downstream IRF4 effector is B-lymphocyte-induced maturation protein-1 (BLIMP-1);<sup>9</sup> indeed, knockdown of BLIMP-1 causes apoptosis in MM cells. These findings suggest that IRF4 may regulate MM cell survival through modulation of BLIMP-1.<sup>9</sup> Moreover, it has been recently demonstrated that caspase-10

(casp-10) and cFlip genes are transactivated by IRF4: importantly, the evidence that all MM cell lines require casp-10 and cFLIP for survival led to the hypothesis that loss of the proteolytic activity of the casp-10/cFlip heterodimer mediates MM cell death induced by IRF4 knockdown.<sup>10</sup> All these data indicate IRF4 as an attractive therapeutic target in MM. However, efficient *in vivo* strategies aimed at blocking IRF4 pathway are still lacking.

MicroRNAs (miRNAs) are small non-coding RNAs of 19–25 nucleotides, which regulate gene expression by degrading or inhibiting translation of target mRNAs, primarily via base pairing to partially or fully complementary sites in the 3′ untranslated region (UTR).<sup>11</sup> Targeting deregulated miRNAs in cancer cells is emerging as a novel promising therapeutic approach,<sup>12–14</sup> including in MM.<sup>15–34</sup> In this scenario, replacement of tumor-suppressor miRNAs by synthetic oligonucleotides (miRNA mimics) offers a new therapeutic opportunity to restore a loss-of-function in cancer, that has been an unmet need for drug developers.<sup>35</sup>

Here, we show that IRF4 expression is regulated by microRNA-125b-5p (miR-125b-5p) in patient-derived MM cells and MM cell lines. In most of these cells, enforced expression of miR-125b-5p affects growth and survival, acting via IRF4 downregulation and impairment of its downstream signaling. Overall, our findings demonstrate that miR-125b is a tumor suppressor in MM, and provide the rationale for development of miR-125b-5p mimics as novel therapeutics.

<sup>1</sup>Department of Experimental and Clinical Medicine, Magna Graecia University, Salvatore Venuta University Campus, Catanzaro, Italy; <sup>2</sup>Department of Medical Sciences, University of Milan, Hematology 1, IRCCS Policlinico Foundation, Milan, Italy; <sup>3</sup>Jerome Lipper Multiple Myeloma Center, Department of Medical Oncology, Dana-Farber Cancer Institute, Boston, MA, USA; <sup>4</sup>VA Boston Healthcare System, West Roxbury, Boston, MA, USA and <sup>5</sup>Sbarro Institute for Cancer Research and Molecular Medicine, Center for Biotechnology, College of Science and Technology, Temple University, Philadelphia, PA, USA. Correspondence: Professor P Tassone, Department of Experimental and Clinical Medicine, Medical Oncology, Magna Graecia University, Viale Europa, Catanzaro 88100, Italy.

E-mail: tassone@unicz.it

Received 19 February 2015; revised 27 April 2015; accepted 5 May 2015; accepted article preview online 19 May 2015; advance online publication, 7 July 2015

## MATERIALS AND METHODS

### MM patient cells and cell lines

Following the Magna Graecia University IRB study approval, primary MM cells were isolated from bone marrow (BM) aspirates, as described,<sup>19</sup> from 24 newly diagnosed MM patients who had provided the informed consent. For transfection purposes and proliferation/survival assays, peripheral blood mononuclear cells (PBMCs) from healthy donors have been used as controls. MM cell lines were cultured as described.<sup>19</sup> HS-5 human stromal cell line (purchased from ATCC, Manassas, VA, USA, CRL-11882) was cultured in Dulbecco's Modified Eagle Medium supplemented with 10% fetal bovine serum and 1% penicillin/streptomycin (see Supplementary Methods for detailed information).

### Virus generation and infection of cells

Cells stably expressing green fluorescent protein transgene were obtained as described.<sup>21</sup> To generate cells stably expressing luciferase transgene, NCI-H929 cells were transduced with pLenti-III-PGK-Luc (ABM Inc., Richmond, BC, Canada) vector. MM cells stably expressing miR-125b-1 and miR-125b-2 genes were transduced with Lenti-miR-125b-1 and Lenti-miR-125b-2 miRNA precursor constructs (System Biosciences, CA, USA); lentiviral particles were produced and transduced as previously described.<sup>19</sup>

### RNA extraction and qRT-PCR.

RNA samples of healthy donors BM-derived plasma cells were purchased (AllCells LLC, Alameda, CA, USA). Total RNA extraction from MM cells and quantitative real-time PCR were performed as previously described (see Supplementary Methods for detailed information).<sup>19</sup>

### *In vitro* transfection of MM cells

Synthetic miRNA mimics were purchased from Ambion (Applied Biosystems, Carlsbad, CA, USA), while synthetic miRNA inhibitors were purchased from Exiqon (Vedbaek, Rudersdal, Denmark). Silencer Select siRNAs were purchased from Ambion (Applied Biosystems). All the oligos were used at 100 nmol/l final concentration. A total of  $2.5 \times 10^5$  cells were transfected using Neon Transfection System (Invitrogen, Carlsbad, CA, USA) (2 pulse at 1.050 V, 30 ms) and the transfection efficiency, evaluated by flow-cytometric analysis relative to a FAM dye-labeled miRNA inhibitor negative control, reached 85 to 90%. The same conditions were applied for transfection of MM cells with 5 µg of expression vectors carrying the open reading frames (ORFs) of BLIMP-1 (EX-Z5827-M11), IRF4 (EX-M0891-M11) or empty vector (EX-EGFP-M11) (GeneCopeia, Rockville, MD, USA).

### Survival assay

Cell viability was evaluated by Cell Counting Kit-8 (CCK-8) assay (Dojindo Molecular Technologies, Mashikimachi, Japan) and 7-Aminoactinomycin (7-AAD) flow cytometry assay (BD Biosciences, San Jose, CA, USA), according to manufacturer's instructions.

### Detection of apoptosis

Apoptosis was investigated by three different assays: Annexin V/7-AAD flow cytometry assay, terminal-deoxynucleotidyl transferase-dUTP nick end labeling (TUNEL) assay and western blot analysis of caspases expression and cleavage. To perform TUNEL assay, transfected cells were fixed using 4% paraformaldehyde and then permeabilized using 0.25% Triton X-100, according to manufacturer's instructions. Cells were stained with a TUNEL assay (Click-iT TUNEL Alexa Fluor 594 Imaging Assay, Invitrogen, 10246) to identify those with fragmented DNA. Nuclei were counterstained with Hoechst 33342 (Life Technologies, CA, USA). Image acquisition was done using EVOS FLOID (Life Technologies) equipped with a 20× Nikon objective.

### Western blot analysis

Whole cell protein extracts were prepared from MM cell lines and from PBMCs in NP40 CellLysis Buffer (Life Technologies) containing a cocktail of protease inhibitors (Sigma, Steinheim, Germany). Cell lysates were loaded and polyacrylamide gel electrophoresis separated. Proteins were transferred by Trans-Blot Turbo Transfer Starter System (Bio-Rad, Hercules, CA, USA) for 7 min. After protein transfer, the membranes were blotted with the primary antibodies (see Supplementary methods for detailed information).

### Animals and *in vivo* model of human MM

Male CB-17 Severe Combined Immunodeficient (SCID) mice (6–8 weeks old; Harlan Laboratories, Inc., Indianapolis, IN, USA) were housed and monitored in our Animal Research Facility. Experimental procedures and protocols had been approved by the Magna Graecia University IRB and conducted according to protocols approved by the National Directorate of Veterinary Services (Italy, Rome). Mice were s.c. inoculated with  $5 \times 10^6$  NCI-H929 cells and treatment started when palpable tumors became detectable. Sample size (that is, number of animals to be inoculated with MM cells) was chosen accordingly to our experience.<sup>16–20</sup> Tumor sizes were measured as described,<sup>19</sup> and the investigator was blinded to group allocation. Tumor size of luciferase gene-marked NCI-H929 xenografts was also measured by IVIS Lumina II (PerkinElmer, Waltham, MA, USA). Oligos were NLE-formulated within MaxSuppressor *In Vivo* LANCer II (Bilo Scientific, Austin, TX, USA) to achieve an efficient delivery, as reported.<sup>16,27</sup>

### Statistical analysis

Each experiment was performed at least three times and values are reported as mean ± s.d. Comparisons between groups were made with student's *t*-test, while statistical significance of differences among multiple groups was determined by GraphPad software (www.graphpad.com). Graphs were obtained using Graphpad Prism version 6.0 (GraphPad Software, La Jolla, CA, USA). *P*-value < 0.05 was accepted as statistically significant.

## RESULTS

### Inverse correlation between IRF4 mRNA and miR-125b in MM patients

To identify IRF4-targeting miRNAs, we interrogated microRNA Data Integration Portal (mirDIP), applying the *high precision* quality

**Table 1.** *In silico* search for IRF4-targeting miRNAs

Gene	MicroRNA	Source	Score (s.d.)
IRF4	hsa-mir-125a-5p	picTar_ver2_hg18_Mar2006_mammals	4.52261
IRF4	hsa-mir-125b-5p	picTar_ver2_hg18_Mar2006_mammals	5.02513
IRF4	hsa-mir-128	picTar_ver2_hg18_Mar2006_mammals	3.51759
IRF4	hsa-mir-27a-3p	picTar_ver2_hg18_Mar2006_mammals	5.02513
IRF4	hsa-mir-27b-3p	picTar_ver2_hg18_Mar2006_mammals	6.03015
IRF4	hsa-mir-30a-5p	picTar_ver2_hg18_Mar2006_mammals	2.01005
IRF4	hsa-mir-30b-5p	picTar_ver2_hg18_Mar2006_mammals	1.00503
IRF4	hsa-mir-30c-2	picTar_ver2_hg18_Mar2006_mammals	1.00503
IRF4	hsa-mir-30d-5p	picTar_ver2_hg18_Mar2006_mammals	2.51256
IRF4	hsa-mir-30e-5p	picTar_ver2_hg18_Mar2006_mammals	4.52261
IRF4	hsa-mir-4319	picTar_ver2_hg18_Mar2006_mammals	14.5729
IRF4	hsa-mir-513a-5p	picTar_ver2_hg18_Mar2006_mammals	14.0704

Abbreviations: IRF4, interferon regulatory factor; miRNA, microRNA.

filter.<sup>36</sup> As shown in Table 1, this analysis disclosed 12 mature miRNAs including miR-125a-5p, miR-125b-5p, miR-128, miR-27a-3p, miR-27b-3p, miR-30a-5p, miR-30b-5p, miR-30c-2, miR-30d-5p, miR-30e-5p, miR-4319 and miR-513a-5p. We next attempted to correlate the expression of these miRNAs and IRF4 mRNA in our dataset (55 MM and 21 plasma cell leukemia patients)(GSE39925). This integrated approach revealed a significant inverse correlation between IRF4 mRNA and five precursor-miRNAs (pre-miR-125b-1, pre-miR-125b-2, pre-miR-30b, pre-miR-30c-2 and pre-miR-30d) among all MM and plasma cell leukemia patients examined (Figures 1a and b and Supplementary Fig. S1A). Importantly, when a second dataset (GSE47552) was interrogated, the inverse correlation with IRF4 mRNA was confirmed only for pre-miR-125b-1 (Supplementary Fig. S1B), strengthening a possible role of miR-125b-5p as IRF4 negative regulator in MM patients. By qRT-PCR, we then evaluated the expression of miR-125b-5p in 24 CD138<sup>+</sup> primary patient MM (ppMM) cells, 10 MM cell lines and 3 samples of CD138<sup>+</sup> BM-derived plasma cells from healthy donors (HD-PCs). A significant downregulation of miR-125b-5p was found in MM cell lines (Figure 1c, with single values plotted in Supplementary Fig. S2), while the downregulatory trend observed in ppMM cells reached statistical significance within the TC2 and TC3 subgroups only (Figures 1c and d).

#### Enforced expression of miR-125b impairs growth and survival of MM cells

To evaluate the effects induced by miR-125b, we transduced 3 MM cell lines (NCI-H929, SK-MM-1, RPMI-8226) with lentiviral vectors carrying either miR-125b-1 or miR-125b-2 (Lenti-miR-125b-1 or Lenti-miR-125b-2) genes. The effects on cell proliferation were assessed by CCK-8 assay at 2, 3 and 4 days after selection by

puromycin. As shown in Figures 2a and b, constitutive expression of either Lenti-miR-125b-1 or Lenti-miR-125b-2 resulted in a strong inhibition of cell growth. Next, we transfected MM cell lines with either synthetic miR-125b-5p mimics or inhibitors. We found that ectopic expression of miR-125b-5p inhibitors did not affect the proliferation of MM cells (Figures 2c and d); conversely, transfection of miR-125b-5p mimics strongly impaired growth and survival of most MM cell lines (9 out of 10) (Figures 2e and f). Importantly, miR-125b-5p mimics reduced the viability of ppMM cells from 3 individuals (Figure 2g), but not of PBMCs from 6 healthy donors (Figure 2h). Taken together, these results indicate that enforced expression of miR-125b-5p inhibits growth and survival of MM cells, consistent with a tumor-suppressor function of this miRNA. Notably, baseline expression of miR-125b-5p did not correlate with the sensitivity/response to synthetic mimics or inhibitors, suggesting that miR-125b-5p expression is not predictive of *in vitro* anti-MM activity. Furthermore, miR-125b-5p mimics were lethal to MM cells irrespective of their genetics.

#### miR-125b-5p mimics inhibit proliferation of MM cells via targeting IRF4

To investigate whether IRF4 expression could be affected by ectopic miR-125b-5p, both qRT-PCR and western blot analysis were performed in 3 MM cell lines transfected with miR-125b-5p mimics or scrambled controls (miR-NC). Specifically, the IRF4 translocated SK-MM-1, along with NCI-H929 and RPMI-8226 cells (not IRF4 translocated), were selected for this analysis. As shown in Figures 3a and b, transfection of miR-125b-5p downregulated IRF4 at both mRNA and protein levels in all MM cell lines. Notably, the only MM cell line resistant to miR-125b-5p overexpression lacked detectable IRF4 (i.e. RPMI-8226/Dox40 cells, which were

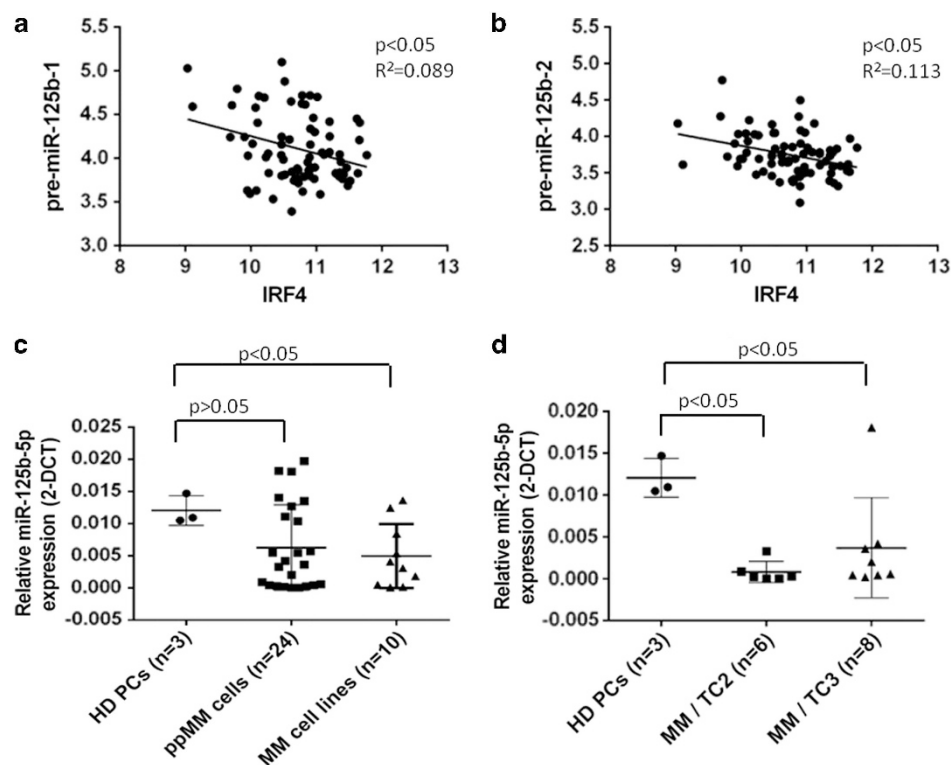
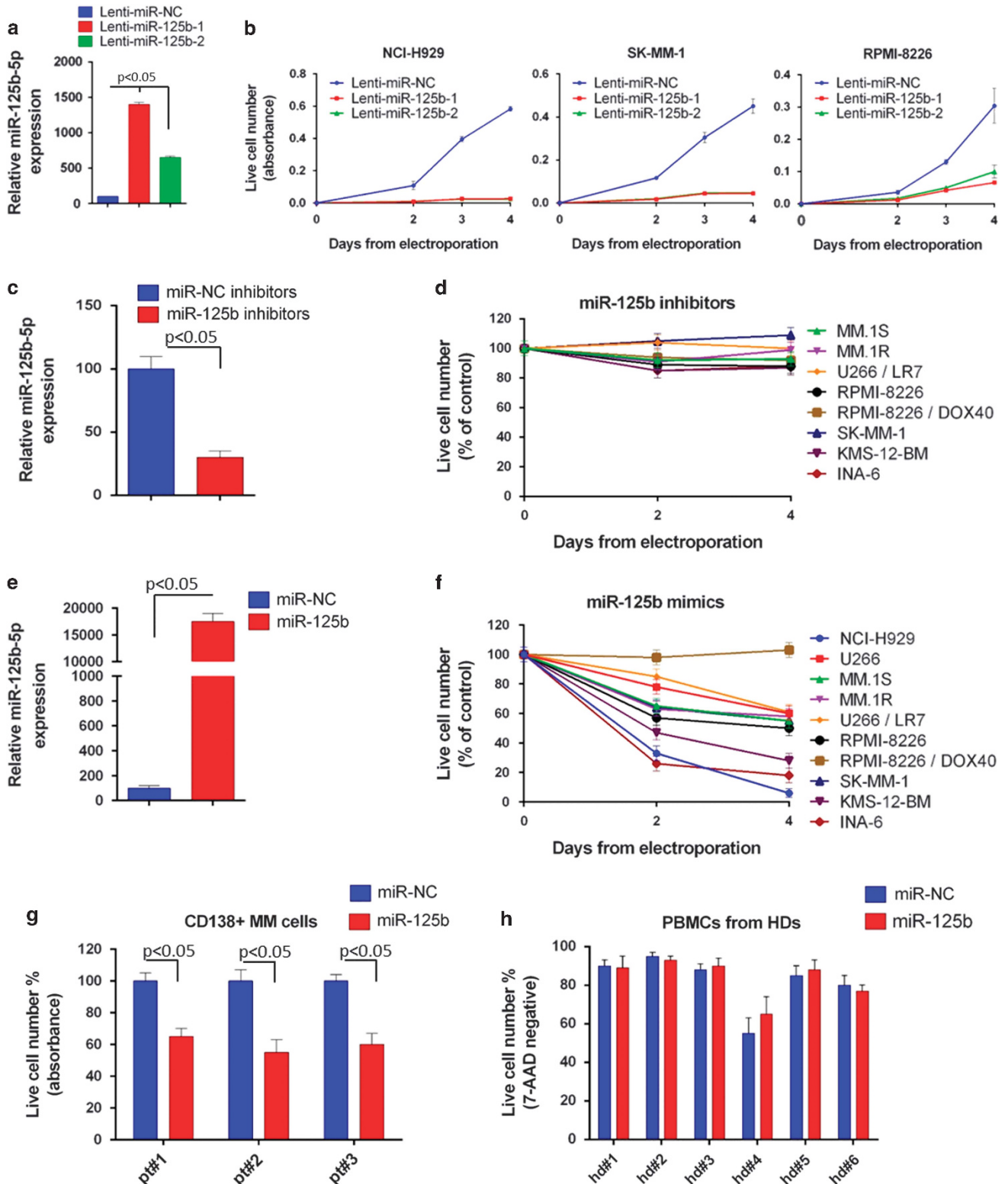


**Figure 1.** miR-125b inversely correlates with IRF4 mRNA in MM patients. Analysis of IRF4 mRNA and either (a) miR-125b-1 or (b) miR-125b-2 expression levels in patient's multiple myeloma cells from published data set GSE39925. (c) qRT-PCR analysis of miR-125b-5p expression using total RNA from 24 primary patient MM cells, 10 MM cell lines and 3 samples of bone marrow-derived plasma cells from healthy donors (HD PCs). (d) MMs were TC classified according to the presence of recurrent IGH chromosomal translocations and Cyclin D expression as previously described,<sup>19</sup> and miR-125b-5p expression in TC2 and TC3 subgroups is plotted. Raw Ct values were normalized to RNU44 housekeeping snoRNA and expressed as  $2^{-\Delta Ct}$  values. Values represent mean  $\pm$  s.e. of three different experiments.

generated from the parental RPMI-8226 by continuous exposure to increasing amounts of doxorubicin to culture medium, is characterized by loss of miR-125b-5p relevant targets) (Supplementary Fig. S3A). Consistently, we found that viability of RPMI-8226/Dox40 cells was not affected by IRF4 siRNA silencing (Supplementary Fig. S3B); in contrast, siRNA-transfection of both NCI-H929 and SK-MM-1 cells confirmed its role in supporting their

survival (Supplementary Fig. S3B). We next investigated whether ectopic expression of a cDNA containing only the coding region of IRF4 and lacking the miR-125b-5p-targeted 3' UTR could protect MM cells from miR-125b-5p anti-proliferative effects. As shown in Figure 3c, transfection of IRF4 construct increased IRF4 protein expression which was not affected by miR-125b-5p mimics. Importantly, IRF4 overexpression rescued SK-MM-1 cells from the





growth-inhibitory activity of either IRF4 siRNAs (Supplementary Fig. S3C) or miR-125b-5p mimics (Figure 3d), indicating that miR-125b-5p exerts its anti-MM activity via targeting IRF4.

#### Enforced expression of miR-125b-5p impairs IRF4 signaling in MM cell lines

We next investigated the effects of miR-125b-5p on the molecular network underlying IRF4 activity in MM. Interestingly, the IRF4-downstream effector BLIMP-1 has been proven to be a direct target of miR-125b-5p.<sup>37</sup> As shown in Figure 4a and Supplementary Fig. S4A, transfection of miR-125b-5p mimics downregulated BLIMP-1 protein in SK-MM-1 and NCI-H929 cells. Thus, we investigated whether ectopic expression of a cDNA containing only the coding region of BLIMP-1 and lacking the miR-125b-5p-targeted 3' UTR could protect MM cells from miR-125b-5p effects. Importantly, co-transfection with BLIMP-1 construct weakened the anti-proliferative effect of miR-125b-5p mimics as well of BLIMP-1 siRNAs (Figure 4c and Supplementary Fig. S4B), indicating that also BLIMP-1 mediates the anti-MM activity of miR-125b-5p. Of note, miR-125b-5p-induced downregulation of BLIMP-1 was not abrogated in SK-MM-1 cells co-transfected with the coding region of IRF4 (Figure 4b), consistent with the notion that BLIMP-1 is a direct target of

miR-125b-5p which circumvents IRF4 activity on BLIMP-1. Other IRF4-downstream effectors, with a prominent role in MM pathogenesis, are c-Myc, casp-10 and cFLIP.<sup>8,10</sup> By western blot analysis, we found reduced expression of these proteins in SK-MM-1 (Figure 4d) and NCI-H929 (Supplementary Fig. S4E) cells at 24–48 h after transfection with miR-125b-5p. Expression of both casp-10 and cFlip was also reduced at mRNA levels (Supplementary Fig. S4F) by miR-125b-5p mimics. *In silico* search for target prediction identified both casp-10 and cFlip as *bona fide* direct targets for miR-125b-5p. To validate this interaction in MM cells, SK-MM-1 cells were co-transfected with miR-125b-5p mimics or scrambled oligonucleotides, together with an expression vector carrying the 3' UTR of casp-10 or cFlip mRNA cloned downstream of luciferase reporter gene. Of note, we did not find significant changes in 3' UTR luciferase activity after miR-125b-5p overexpression, ruling out direct targeting of casp-10 and cFlip mRNAs by miR-125b-5p (Supplementary Fig. S4G). Moreover, miR-125b-5p-induced downregulation of c-Myc, casp-10 and cFlip was abrogated in SK-MM-1 cells co-transfected with the coding region of IRF4 (Figure 4e), indicating that miR-125b-5p-induced downregulation of casp-10, c-Myc and cFlip occurs via IRF4 inhibition. Taken together, our findings demonstrate that miR-125b-5p mimics impair IRF4 signaling in MM cells (Figure 4f). We also found that direct targeting

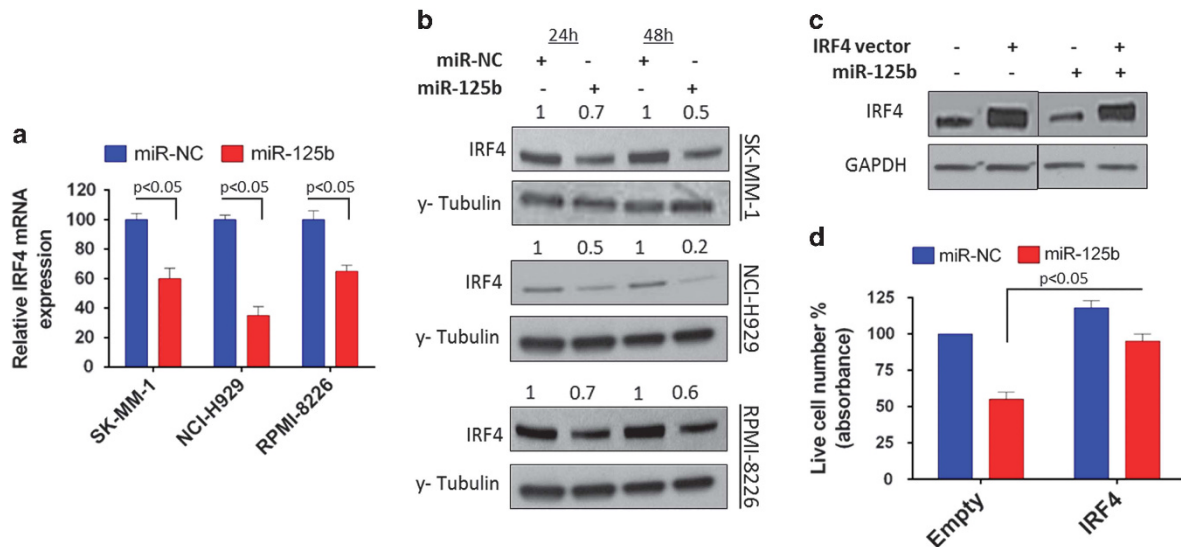


**Figure 3.** IRF4 downregulation mediates miR-125b-5p anti-MM activity. **(a)** qRT-PCR analysis of IRF4 expression in SK-MM-1, NCI-H929 and RPMI-8226 cells 48 h after transfection with miR-125b-5p or miR-NC. The results shown are average mRNA expression levels after normalization with GAPDH and  $\Delta\Delta C_t$  calculations. **(b)** Western blot analysis of IRF4 in SK-MM-1, NCI-H929 and RPMI-8226 cells transfected with miR-125b-5p or miR-NC. Analysis was performed 24 and 48 h after cell transfection.  $\gamma$ -Tubulin was used as protein loading control. **(c)** Western blot analysis of IRF4 in lysates from SK-MM-1 cells co-transfected with either IRF4 ORF expression vector or an empty vector and miR-125b-5p or miR-NC (48-h time point). **(d)** CCK-8 assay of SK-MM-1 cells co-transfected with either IRF4 ORF expression vector or an empty vector and miR-125b-5p or miR-NC (72-h time point). Data represent the average  $\pm$  s.d. of three independent experiments.

**Figure 2.** Anti-proliferative effects of miR-125b in MM cells. **(a)** qRT-PCR analysis of miR-125b-5p expression in SK-MM-1 cells transduced with either Lenti-miR-125b-1 or Lenti-miR-125b-2; the results are shown as average miR-125b-5p expression levels after normalization with RNU44 and  $\Delta\Delta C_t$  calculations. **(b)** CCK-8 proliferation assay of NCI-H929, SK-MM-1 and RPMI-8226 cells transduced with a lentivirus carrying either the miR-125b-1 (Lenti-miR-125b-1) or the miR-125b-2 (Lenti-miR-125b-2) genes; the effects on cell proliferation were assessed at 2, 3 and 4 days after selection by puromycin. qRT-PCR analysis of miR-125b-5p expression in SK-MM-1 cells transfected with either **(c)** miR-125b-5p inhibitors or **(e)** miR-125b-5p mimics; the results are shown as average miR-125b-5p expression levels after normalization with RNU44 and  $\Delta\Delta C_t$  calculations. **(d)** CCK-8 proliferation assay was performed 2–4 days after transfection of eight MM cell lines (MM.1S, MM.1R, U266/LR7, RPMI-8226, RPMI-8226/DOX40, SK-MM-1, KMS-12-BM and INA-6) with miR-125b-5p inhibitors or scrambled controls (miR-NC inhibitors). **(f)** CCK-8 proliferation assay was performed 2–4 days after transfection of 10 MM cell lines (NCI-H929, U266, MM.1S, MM.1R, U266/LR7, RPMI-8226, RPMI-8226/DOX40, SK-MM-1, KMS-12-BM and INA-6) with miR-125b-5p mimics or scrambled controls (miR-NC mimics). **(g)** CCK-8 assay of CD138+ cells from three different MM patients transfected with miR-125b-5p or miR-NC. The assay was performed 48 h after cell transfection. **(h)** 7-AAD flow cytometry assay was performed 48 h after transfection of PBMCs from six healthy donors (HDs) with miR-125b-5p or miR-NC. Data represent the average  $\pm$  s.d. of three independent experiments. *P*-values were obtained using two-tailed *t*-test.

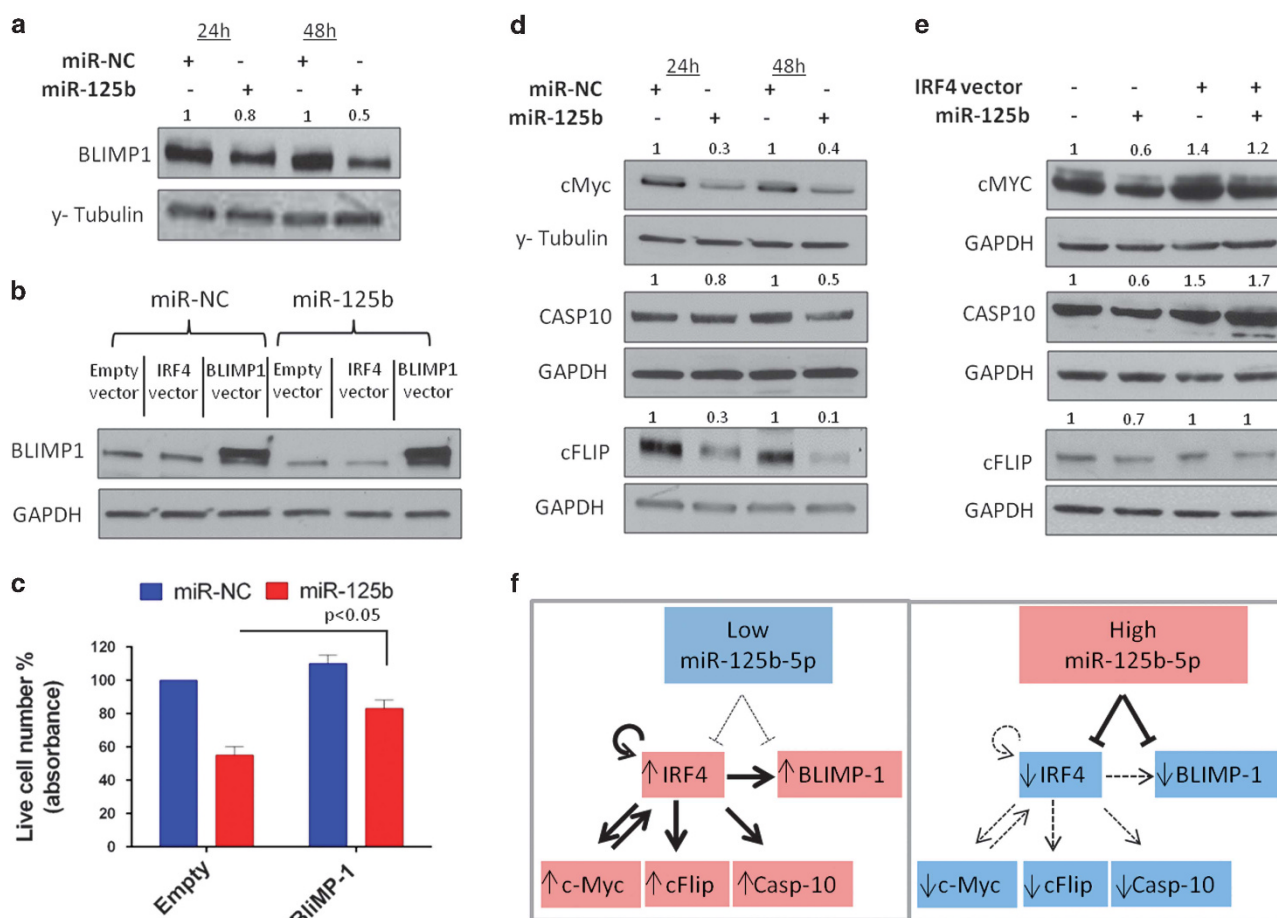


**Figure 4.** Impairment of IRF4 signaling by miR-125b-5p. **(a)** Western blot analysis of BLIMP-1 in SK-MM-1 cells transfected with miR-125b-5p or miR-NC. Analysis was performed 24 and 48 h after cell transfection.  $\gamma$ -Tubulin was used as protein loading control. **(b)** Western blot analysis of BLIMP-1 in lysates from SK-MM-1 cells co-transfected with either BLIMP-1 ORF expression vector or an empty vector and miR-125b-5p or miR-NC (48-h time point). **(c)** CCK-8 assay of SK-MM-1 cells co-transfected with either BLIMP-1 ORF expression vector or an empty vector and miR-125b-5p or miR-NC (72-h time point). **(d)** Western blot analysis of c-Myc, Casp-10 and cFLIP in SK-MM-1 cells transfected with miR-125b-5p or miR-NC. Analysis was performed 24 and 48 h after cell transfection. GAPDH or  $\gamma$ -Tubulin were used as protein loading controls. **(e)** Western blot analysis of c-Myc, Casp-10 and cFLIP in lysates from SK-MM-1 cells co-transfected with either IRF4 ORF expression vector or an empty vector and miR-125b-5p or miR-NC (48-h time point). GAPDH was used as protein loading control. All the experiments were performed in triplicate. Representative pictures are shown. **(f)** Explanatory cartoon of miR-125b-5p-mediated impairment of IRF4 signaling.

of IRF4 or BLIMP-1 and indirect modulation of c-Myc, casp-10 and cFlip mediates anti-MM activity of this miRNA.

#### miR-125b-5p mimics trigger both apoptotic and autophagy-associated cell death

Inhibition of IRF4, as well of BLIMP-1 or c-Myc, has been mainly related to induction of apoptosis,<sup>9,38</sup> while targeting casp-10 or its interaction with cFlip triggers autophagic cell death of MM cells.<sup>10</sup> On this basis, we next determined whether apoptotic or autophagy-associated cell death occurred in MM cells with enforced expression of miR-125b-5p. Using Annexin V/7-AAD flow cytometry assay, we found that miR-125b-5p mimics triggered exposure of phosphatidylserine (PS) and phosphatidylethanolamine (PE) on the cell surface of SK-MM-1 (Figure 5a), NCI-H929 and U266 cells (Supplementary Fig. S5A), followed by cell membrane disruption. Moreover, by TUNEL assay and western blotting, we found that miR-125b-5p induced DNA-fragmentation (Supplementary Fig. S5B) and cleavage/activation of both initiator casp-8 and effector casp-3 (Figure 5b and Supplementary Fig. S5C) in MM cells. Of note, apoptosis was not detected when miR-125b-5p-transfected cells were treated with the pan-caspase inhibitor Z-VAD-fmk (Figure 5c). Overall, these results indicate that

miR-125b-5p is pro-apoptotic in MM cells. Moreover, by flow cytometry analysis of Cyto-ID stained cells, we observed an increase of autophagic vacuoles in SK-MM-1, XG-1 and INA-6 cells, at 48 h after transfection with miR-125b-5p (Figure 5d). Importantly, the increase of autophagic vacuoles occurred to a similar extent in cells transfected with miR-125b-5p compared with cells starved for 48 h. Moreover, western blot analysis showed decreased p-62/SQSTM1 and increased Beclin-1 and proteolytic active LCIIIb (Figure 5e), further indicating that miR-125b-5p-induced cell death can be associated with autophagy induction in MM cells. Indeed, exposure of miR-125b-5p-transfected cells to autophagy inhibitor cloroquine resulted in increased cell death (Figure 5f), thus suggesting a protective role of autophagy in our experimental settings.

#### miR-125b-5p mimics antagonize the BMSCs protective role on MM cells

BM milieu strongly supports survival and proliferation of MM cells.<sup>3</sup> In this regard, we found that exogenous interleukin-6 (IL-6) or insulin-like growth-factor-1 (IGF-1) or hepatocyte growth-factor (HGF) significantly reduced miR-125b-5p expression in all MM cell lines except U266 cells (Figure 6a), which express L-Myc instead of

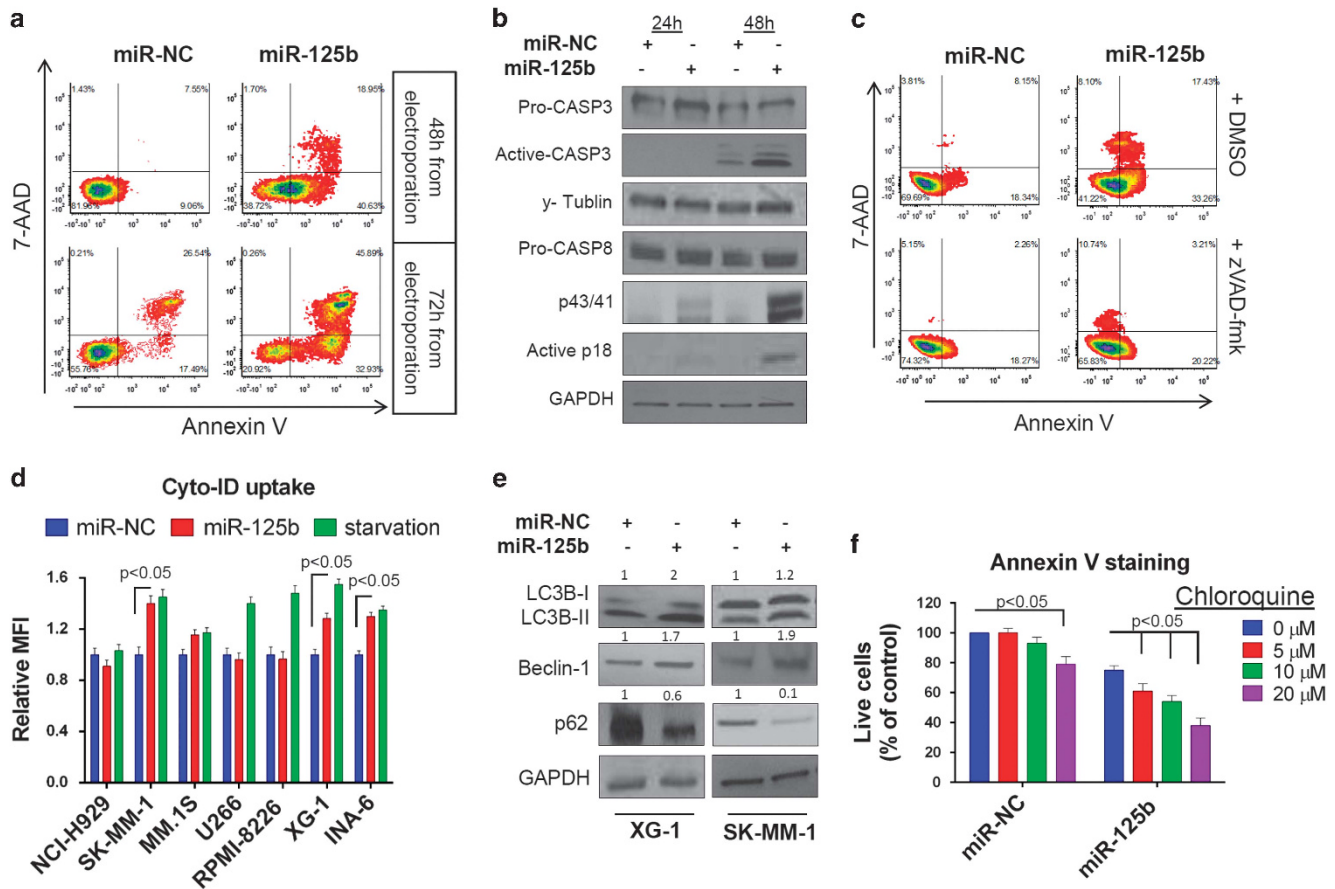


**Figure 5.** miR-125b-5p increases both apoptosis and autophagic efflux in MM cells. **(a)** Annexin V/7-AAD staining of SK-MM-1 cells transfected with miR-125b-5p or miR-NC. Flow cytometry analysis was performed 48–72 h after transfection. **(b)** Western blot analysis of casp-3 and casp-8 activities in SK-MM-1 cells transfected with miR-125b-5p mimics or miR-NC. Analysis was performed 24–48 h after cell transfection.  $\gamma$ -Tubulin or GAPDH were used as protein loading controls. **(c)** Annexin V/7-AAD staining of SK-MM-1 cells transfected with miR-125b-5p or miR-NC. Six hours after electroporation either DMSO or zVAD-fmk were added to culture medium, at final concentration of 25  $\mu$ M. Flow cytometry analysis was performed 48 h after transfection. **(d)** Cyto-ID uptake flow cytometry assay was performed in seven MM cell lines (NCI-H929, SK-MM-1, MM-1S, U266, RPMI-8226, XG-1 and INA-6) 48 h after transfection with miR-125b-5p or miR-NC. **(e)** Western blot analysis of LC3B, Beclin-1 and p-62 was performed in XG-1 and SK-MM-1 cells transfected with miR-125b-5p or miR-NC. Analysis of LC3B and Beclin-1 was performed 24 h after cell transfection, while analysis of p-62 was performed 48 h after cell transfection. GAPDH was used as a protein loading control. **(f)** Annexin V/7-AAD staining of SK-MM-1 cells transfected with miR-125b-5p or miR-NC and then exposed to increasing concentrations (0, 5, 10 and 20  $\mu$ M) of the autophagy inhibitor chloroquine (added to culture medium 6 h after electroporation). Flow cytometry analysis was performed 72 h after transfection. All the experiments were performed in triplicate. Representative pictures are shown.

c-Myc. Since c-Myc suppresses miR-125b transcription<sup>39,40</sup> and is upregulated by IL-6, IGF-1 and HGF,<sup>40–42</sup> we investigated whether these factors downregulate miR-125b in MM cells through c-Myc induction. Specifically, we treated c-Myc-expressing SK-MM-1 and c-Myc-defective U266 cells with the 10058-F4 small molecule inhibitor of Myc–Max heterodimerization<sup>38</sup> and with the JQ1 BET-bromodomain inhibitor, which is reported to inhibit c-Myc transcription.<sup>43</sup> Importantly, both compounds triggered a significant miR-125b-5p upregulation in SK-MM-1 cells, but not in U266 cells (Figure 6b), indicating that c-Myc-independent downregulation of miR-125b occurs in this cell line. Moreover, IL-6 or IGF-1 or HGF did not affect miR-125b-5p expression in SK-MM-1 cells in the presence of c-Myc inhibitors, indicating a c-Myc-mediated downregulation of miR-125b by exogenous addition of microenvironmental growth factors (Figure 6c). Finally, we demonstrated that the anti-MM activity of miR-125b-5p mimics was not antagonized by exogenous growth promoting/pro-survival stimuli including IL-6, IGF-1 and HGF, or by adherence of MM cell lines to HS-5 human stromal cells (Figures 6d and e). This could be partly due to downregulation of IL-6R/CD126 on the surface of MM cells. Indeed, by flow cytometry analysis, we did observe decreased expression of cell surface IL-6R/

CD126, also a further validated target of miR-125b-5p<sup>44</sup> (Figure 6f), which translated in reduced levels of phosphorylated/active STAT3 (pSTAT3-Y705) in IL-6-dependent INA-6 cells (Figure 6g).

*In vivo* delivery of NLE-formulated synthetic miR-125b-5p mimics exerts anti-MM activity

*In vivo* anti-MM activity of miR-125b-5p was next evaluated in Non-Obese Diabetic (NOD)/SCID mice bearing subcutaneous NCI-H929 xenografts. In our first model, luciferase gene-marked NCI-H929 xenografts were intra-tumorally treated every other day with 1 mg/kg of oligos for a total of six injections. As shown in Figures 7a–c, treatment resulted in a significant tumor-growth inhibition and prolonged survival. In a second model, treatments were administered by i.p. injections of formulated oligos (twice weekly, 1 mg/kg). In this model, we also observed anti-tumor activity of miR-125b-5p, evidenced by growth inhibition and prolonged survival (Figures 7d and e). Importantly, we found increased miR-125b-5p in tumors retrieved from animals 48 h after treatment, confirming efficient tumor cells uptake of formulated oligos (Figure 7f). Consistent with our *in vitro* data, IRF4 signaling



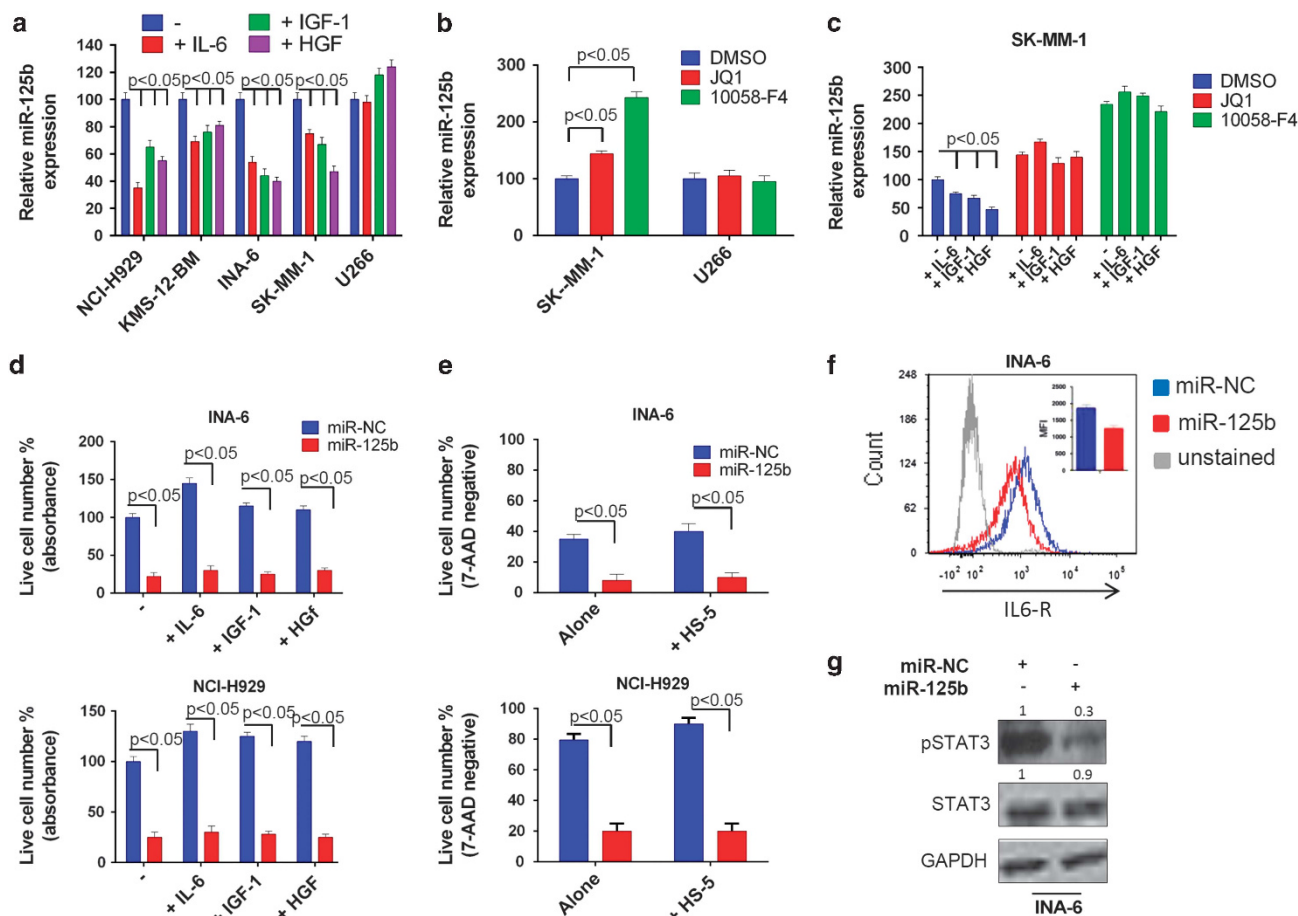


**Figure 6.** miR-125b-5p antagonizes pro-survival effect of BM milieu. (a) Quantitative RT-PCR of miR-125b-5p expression in NCI-H929, KMS-12-BM, INA-6, SK-MM-1 and U266 cells cultured in the presence or absence of either IL-6 (2.5 ng/ml) or IGF-1 (100 µg/ml) or HGF (150 µg/ml) (48-h time point). Raw Ct values were normalized to RNU44 housekeeping snoRNA and expressed as  $\Delta\Delta Ct$  values calculated using the comparative cross threshold method. miR-125b-5p expression levels in cells cultured in the absence of growth factors were set as an internal reference. (b) Quantitative RT-PCR of miR-125b-5p expression in SK-MM-1 and U266 cells exposed to either DMSO or JQ1 (1 µM) or 10058-F4 (100 µM) (48-h time point). Raw Ct values were normalized to RNU44 housekeeping snoRNA and expressed as  $\Delta\Delta Ct$  values calculated using the comparative cross threshold method. miR-125b-5p expression levels in cells exposed to DMSO were set as an internal reference. (c) Quantitative RT-PCR of miR-125b-5p expression in SK-MM-1 cells cultured in the presence or absence of either IL-6 (2.5 ng/ml) or IGF-1 (100 µg/ml) or HGF (150 µg/ml) and exposed to either DMSO or JQ1 (1 µM) or 10058-F4 (100 µM) (48-h time point). Raw Ct values were normalized to RNU44 housekeeping snoRNA and expressed as percentage of  $\Delta\Delta Ct$  values calculated using the comparative cross threshold method. miR-125b-5p expression level in cells cultured in absence of growth factors and exposed to DMSO was set as an internal reference. (d) CCK-8 assay was performed 2 days after transfection of INA-6 and NCI-H929 cells with miR-125b-5p or miR-NC. IL-6 (2.5 ng/ml) or IGF-1 (100 ng/ml) or HGF (150 ng/ml) were added to complete culture medium. (e) 7-AAD flow cytometry assay of INA-6 and NCI-H929 cells cultured in the presence or absence of HS-5/GFP+ stromal cell line. The assay was performed 48 h after transfection of MM cells with miR-125b-5p mimics or miR-NC. To discriminate between MM cells and HS-5 stromal cells, GFP negative cells were gated. (f) Flow cytometry analysis of IL6-R/CD126 expression on cell surface of INA-6 cells after transfection with miR-125b-5p or miR-NC (48-h time point). (g) Western blot analysis of total STAT3 (tSTAT3) and phosphorylated STAT3 (pSTAT3) in lysates from INA-6 cells transfected with miR-125b-5p or miR-NC (48-h time point). GAPDH was used as protein loading control.

was correlated with miR-125b-5p activity *in vivo*: downregulation of IRF4 and BLIMP-1 (Figure 7g), along with decreased expression of c-Myc, casp-10 and cFlip proteins (Figure 7h), was detected in tumors retrieved from miR-125b-5p-treated animals. Overall, these data indicate that *in vivo* anti-MM activity of miR-125b-5p mimics is associated with abrogation of IRF4 signaling within MM xenografts.

## DISCUSSION

In this study, we investigated the anti-MM activity of the IRF4-targeting miR-125b-5p. IRF4 is in fact an 'Achilles' heel' for MM cells and, therefore, represents an attractive therapeutic target in this malignancy.<sup>7</sup> miRNAs are natural antisense interactors of mRNAs, and the availability of suitable *in vivo* delivery systems has

recently allowed the development of synthetic miRNA mimics in early clinical trials. By querying mirDIP<sup>36</sup> and applying the high precision quality filter, we found 12 mature miRNAs predicted to target the 3' UTR of IRF4 mRNA, including miR-125b-5p. Importantly, integrated analysis of miRNAs and mRNAs expression profiles showed that miR-125b, but not the other predicted miRNAs, inversely correlated with IRF4 mRNA in two different MM datasets, strengthening the relevance of miR-125b as IRF4 negative regulator in MM patients. Furthermore, miR-125b-5p was found significantly downregulated in patients belonging to TC2 and TC3 molecular subgroups, as well as in MM cell lines. Altogether, these findings prompted us to investigate the role of this miRNA in MM.

miR-125b is one of the most evolutionary conserved miRNAs.<sup>45</sup> In humans there are two paralogs (hsa-miR-125b-1 on



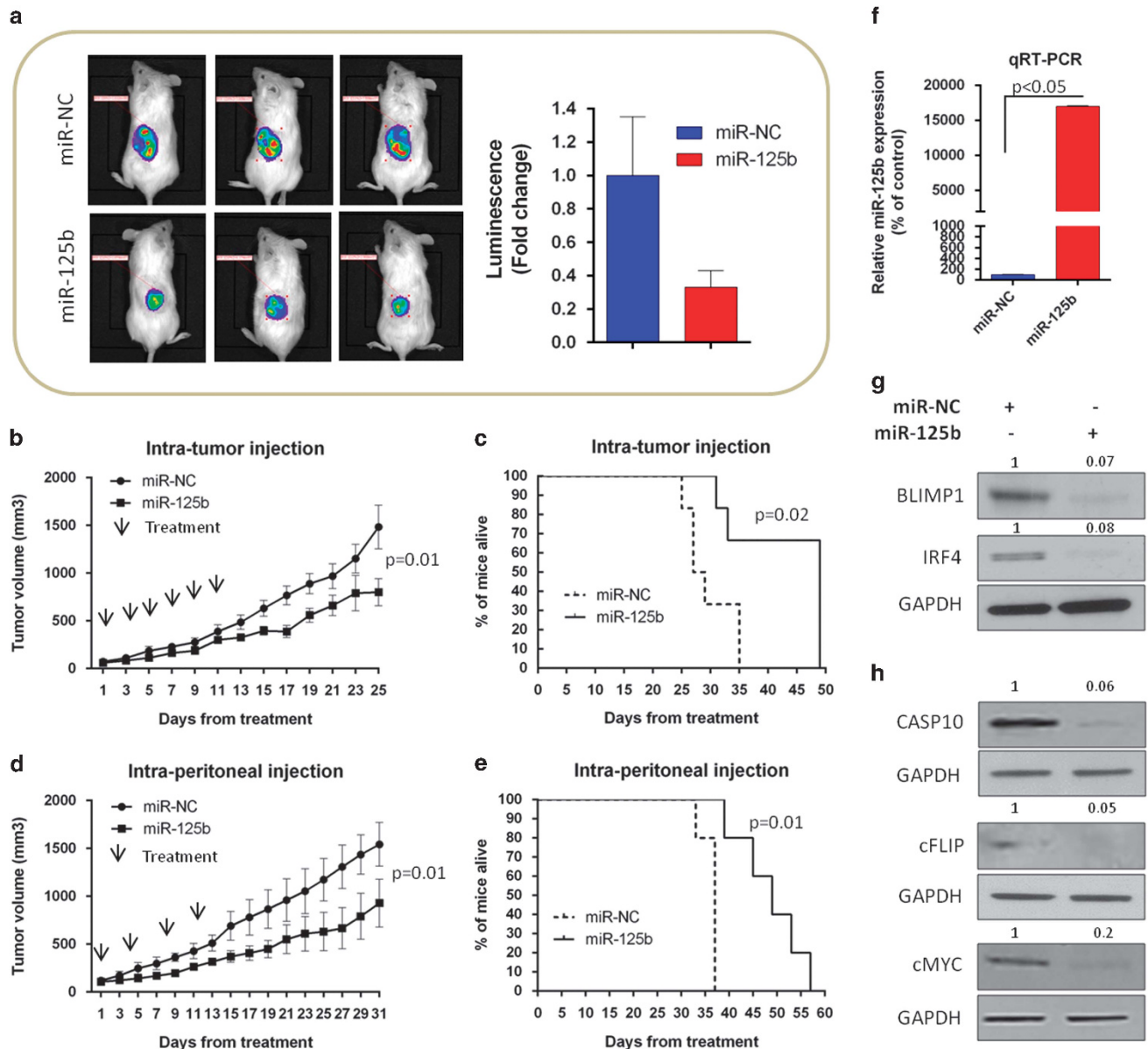


**Figure 7.** miR-125b-5p mimics antagonize MM tumor growth *in vivo*. *In vivo* growth of luciferase gene-marked NCI-H929 xenografts intra-tumorally treated with miR-125b-5p mimics or scr controls. Palpable subcutaneous tumor xenografts were treated with 20  $\mu$ g of NLE-formulated oligos. Intra-tumor injections were administered every other day, for a total of six injections (indicated by arrows). **(a)** BLI-based measurement of tumor volumes (three mice for each group) was made at 25 days from treatment. **(b)** Tumors were also measured with an electronic caliper every other day (five mice for each group). Averaged tumor volume of each group  $\pm$  s.d. is shown. *P*-values were obtained using two-tailed *t*-test. **(c)** Survival curves (Kaplan–Meier) of intra-tumorally treated mice show prolongation of survival in miR-125b-5p-treated NCI-H929 xenografts compared with controls (log-rank test, *P* < 0.05). Survival was evaluated from the first day of treatment until death or sacrifice. Percentage of mice alive is shown. **(d)** *In vivo* tumor growth of NCI-H929 xenografts i.p. treated with NLE-formulated miR-125b-5p or miR-NC. I.p. injections were administered twice weekly, for a total of four injections (indicated by arrows). Tumors were measured with an electronic caliper every other day (five mice for each group). Averaged tumor volume of each group  $\pm$  s.d. is shown. *P*-values were obtained using two-tailed *t*-test. **(e)** Survival curves (Kaplan–Meier) of i.p.-treated mice show prolongation of survival in miR-125b-5p-treated NCI-H929 xenografts compared with controls (log-rank test, *P* < 0.05). Survival was evaluated from the first day of treatment until death or sacrifice. Percentage of mice alive is shown. **(f)** qRT-PCR of miR-125b-5p expression in lysates from retrieved NCI-H929 xenografts intra-tumorally treated with miR-125b-5p or miR-NC. The results shown are average miRNA expression levels after normalization with RNU44 and  $\Delta\Delta$ Ct calculations. Data represent the average  $\pm$  s.d. of three independent experiments. **(g)** Western blot analysis of BLIMP-1 and IRF4 in lysates from a representative retrieved NCI-H929 xenograft intra-tumorally treated with miR-125b-5p or miR-NC. GAPDH was used as protein loading control. **(h)** Western blot analysis of CASP10, cFLIP and c-Myc in lysates from a representative retrieved NCI-H929 xenograft intra-tumorally treated with miR-125b-5p or miR-NC. GAPDH was used as a protein loading control.

chromosome 11 and hsa-miR-125b-2 on chromosome 21), coding for the same mature sequences (miR-125b-5p and miR-125b-3p).<sup>45</sup> miR-125b has a crucial role in a variety of cellular processes and diseases.<sup>46</sup> It is commonly dysregulated in cancer,<sup>46</sup> but its function diverges in different malignancies, with dependence on

the molecular contexts. However, its role in MM is still largely undisclosed.<sup>46–48</sup>

We here provide the evidence that miR-125b acts as a tumor suppressor in MM by targeting IRF4 and BLIMP-1 mRNAs, and importantly we show that NLE-formulated synthetic miR-125b-5p

mimics induce anti-tumor activity *in vivo*. Specifically, we demonstrate that both lentivirus-based constitutive expression of miR-125b-1/-2 genes and transient enforced expression of synthetic miR-125b-5p mimics inhibit the growth and survival of MM cell lines. Moreover, viability of ppMM cells, but not of PBMCs from healthy donors, was affected by transfection with miR-125b-5p mimics, suggesting a favorable therapeutic activity. In our study, baseline expression of miR-125b-5p does not correlate with *in vitro* sensitivity of MM cells to synthetic mimics; consistent with our findings, increasing evidence demonstrate that cancer cells with normal miRNA expression are indeed susceptible to miRNA treatment.<sup>35</sup> Importantly, the anti-MM activity of miR-125b-5p mimics was not affected by either exogenous growth promoting/pro-survival stimuli including IL-6, IGF-1 or HGF, or by adherence of MM cell lines to BM stromal cells (BMSCs). This is a crucial point taking into account that the close and dynamic interplay between MM cells and BMSCs leads to activation of signal transduction pathways which promote cell-cycle progression and protection from apoptosis.<sup>3</sup> Furthermore, a c-Myc-mediated downregulation of miR-125b by exposure of MM cells to different growth factors was observed.

To date, a variety of oncogenic pathways have been identified as directly regulated by miR-125b.<sup>46,47</sup> Here, we demonstrate a functional link between this miRNA and the oncogenic IRF4 signaling in MM. IRF4 is a validated target of miR-125b-5p<sup>37,49</sup> and the relevance of this interaction is well established in both myeloid- and B-cell leukemias, wherein IRF4 acts as a tumor suppressor and miR-125b as a tumor promoter.<sup>50</sup> We found that IRF4 expression was downregulated on transfection of MM cells with miR-125b-5p mimics. Among the MM cell lines studied, only miR-125b-5p-resistant RPMI-8226/Dox40 cells did not express detectable levels of IRF4. Importantly, overexpression of IRF4 was able to rescue SK-MM-1 cells from the growth-inhibitory activity of miR-125b-5p. Altogether, these data indicate that IRF4 mediates the anti-MM activity of miR-125b-5p mimics *in vitro*, underlying a novel and divergent role of miR-125b-5p/IRF4 axis in MM as compared with other hematological malignancies.

miRNAs function as master regulators of the genome by modulating the expression of tens to hundreds of genes, often belonging to the same pathway.<sup>35</sup> This mechanism of action provides advantage to the therapeutic use of miRNAs, since it is consistent with the current vision of cancer as a pathway disease.<sup>35</sup> Interestingly, the IRF4-downstream effector BLIMP-1 is also regulated by miR-125b-5p,<sup>37</sup> and we demonstrated that, similar to IRF4 but to a lesser extent, it also mediates the growth-inhibitory activity of miR-125b-5p. Moreover, we analyzed perturbations occurring in other relevant effectors of IRF4 signaling, including c-Myc, casp-10 and cFlip. c-Myc has a prominent role in the pathogenesis of MM, wherein it represents an attractive therapeutic target.<sup>7,38,43</sup> Importantly, ectopic expression of miR-125b-5p significantly decreased c-Myc protein in MM cells which was rescued by co-transfection with the coding region of IRF4, indicating that IRF4 mediates miR-125b-5p-triggered downregulation of c-Myc. Recently, it has been demonstrated that MM cells further require the IRF4-downstream effectors casp-10 and cFlip for their survival: indeed, the heterodimeric protease composed of casp-10 and cFLIP proteins has a balancing role among the pro-survival and pro-death effects of autophagy.<sup>10</sup> Consistent with these notions, we found that both casp-10 and cFlip undergo significant downregulation on miR-125b-5p ectopic expression in MM cells, along with increased autophagic flux. Nonetheless, the role of autophagy as a response to miR-125b-5p overexpression points to further investigation, taking into account that our present data indeed suggest a protective effect at least in SK-MM-1 cells. Even though *in silico* search for target prediction indicated both casp-10 and cFlip as *bona fide* direct targets for miR-125b-5p, we failed to validate this interaction. However, miR-125b-5p-induced downregulation of casp-10 and cFlip was

abrogated by ectopic IRF4 expression, indicating that miR-125b-5p-mediated downregulation of these two survival factors depends on IRF4 targeting.

Finally, we demonstrated the *in vivo* anti-tumor activity of NLE-formulated miR-125b-5p mimics against human MM xenografts in SCID/NOD mice. To our knowledge, this is the first evidence of a successful *in vivo* treatment with miR-125b-5p mimics in a murine xenograft model of human MM, which indeed has important potential towards clinical applications. We showed that both intra-tumor and i.p. injection of NLE-formulated miR-125b-5p mimics resulted in significant tumor-growth inhibition and prolonged survival. Moreover, in tumors retrieved from animals treated with miR-125b-5p mimics, a downregulation of its direct targets IRF4 and BLIMP-1, along with a reduction in expression of c-Myc, casp-10 and cFlip proteins, was observed. These findings suggest that the *in vivo* anti-MM activity of miR-125b-5p mimics is related to the impairment of IRF4 signaling within MM xenografts. Further *in vivo* evaluation in preclinical models recapitulating the huBMM, such as the SCID-synth-hu,<sup>51</sup> will strengthen the translational value of miR-125b-5p mimics.

We think that our study provides important proof-of-concept findings for the basic strategy of miRNA therapeutics. In fact, we found that the miR-125b-5p/IRF4 axis has a highly disease-specific functional role in MM, which runs in opposite directions as compared with other hematological malignancies. These findings support the peculiarity of MM BM microenvironment disease scenario, which opens highly specific therapeutic avenues. An additional important point is that miR-125b-5p strongly inhibits both IRF4 and BLIMP-1, offering a pathway-directed therapeutic tool, which is still undruggable by alternative approaches. In conclusion, our investigation provides evidence that miR-125b has tumor-suppressor activity in MM and that enforced expression of synthetic miR-125b-5p mimics induces significant anti-MM activity *in vitro* and *in vivo* by IRF4 targeting. Taken together, these results provide the rational framework for development of miR-125b-5p-based therapies in MM.

## CONFLICT OF INTEREST

The authors declare no conflict of interest.

## ACKNOWLEDGEMENTS

This work has been supported by funds of Italian Association for Cancer Research (AIRC), Pt. PT. 'Special Program Molecular Clinical Oncology—5 per mille' n. 9980, 2010/15. This work has also been supported by a grant from NIH PO1-155258, RO1-124929, P50-100007, PO1-78378 and VA merit grant IO1-24467. Nicola Amodio was supported by a 'Fondazione Umberto Veronesi' post-doctoral fellowship.

## AUTHOR CONTRIBUTIONS

EM, EL, MEGC, MTDM, NA, LB, AG, UF, MRP, CB and MR performed experiments and analyzed the data; AN provided biological samples; PT and PT conceived the study; EM, PT and PT wrote the manuscript; NCM and KCA provided critical evaluation of experimental data and manuscript.

## REFERENCES

- Anderson KC, Carrasco RD. Pathogenesis of myeloma. *Annu Rev Pathol* 2011; **6**: 249–274.
- Rajkumar SV. Treatment of multiple myeloma. *Nat Rev Clin Oncol* 2011; **8**: 479–491.
- Podar K, Chauhan D, Anderson KC. Bone marrow microenvironment and the identification of new targets for myeloma therapy. *Leukemia* 2009; **23**: 10–24.
- Rossi M, Di Martino MT, Morelli E, Leotta M, Rizzo A, Grimaldi A et al. Molecular targets for the treatment of multiple myeloma. *Curr Cancer Drug Targets* 2012; **12**: 757–767.
- Morgan GJ, Walker BA, Davies FE. The genetic architecture of multiple myeloma. *Nat Rev Cancer* 2012; **12**: 335–348.

- 6 Kuehl WM, Bergsagel PL. Molecular pathogenesis of multiple myeloma and its premalignant precursor. *J Clin Invest* 2012; **122**: 3456–3463.
- 7 Shaffer AL, Emre NC, Romesser PB, Staudt LM. IRF4: immunity. Malignancy! Therapy? *Clin Cancer Res* 2009; **15**: 2954–2961.
- 8 Shaffer AL, Emre NC, Lamy L, Ngo VN, Wright G, Xiao W *et al*. IRF4 addiction in multiple myeloma. *Nature* 2008; **454**: 226–231.
- 9 Lin FR, Kuo HK, Ying HY, Yang FH, Lin KL. Induction of apoptosis in plasma cells by B lymphocyte-induced maturation protein-1 knockdown. *Cancer Res* 2007; **67**: 11914–11923.
- 10 Lamy L, Ngo VN, Emre NC, Shaffer AL 3rd, Yang Y, Tian E *et al*. Control of autophagic cell death by caspase-10 in multiple myeloma. *Cancer Cell* 2013; **23**: 435–449.
- 11 Bartel DP. MicroRNAs: genomics, biogenesis, mechanism, and function. *Cell* 2004; **116**: 281–297.
- 12 Garzon R, Marcucci G, Croce CM. Targeting microRNAs in cancer: rationale, strategies and challenges. *Nat Rev Drug Discov* 2010; **9**: 775–789.
- 13 Trang P, Weidhaas JB, Slack FJ. MicroRNAs as potential cancer therapeutics. *Oncogene* 2008; **27**: S52–S57.
- 14 Misso G, Di Martino MT, De Rosa G, Farooqi AA, Lombardi A, Campani V *et al*. Mir-34: a new weapon against cancer? *Mol Ther Nucleic Acids* 2014; **3**: e194.
- 15 Amodio N, Di Martino MT, Neri A, Tagliaferri P, Tassone P. Non-coding RNA: a novel opportunity for the personalized treatment of multiple myeloma. *Exp Opin Biol Ther* 2013; **13**: S125–S137.
- 16 Di Martino MT, Leone E, Amodio N, Foresta U, Lionetti M, Pitari MR *et al*. Synthetic miR-34a mimics as a novel therapeutic agent for multiple myeloma: in vitro and in vivo evidence. *Clin Cancer Res* 2012; **18**: 6260–6270.
- 17 Di Martino MT, Gulla A, Gallo Cantafo ME, Altomare E, Amodio N, Leone E *et al*. In vitro and in vivo activity of a novel locked nucleic acid (LNA)-inhibitor-miR-221 against multiple myeloma cells. *PLoS One* 2014; **9**: e89659.
- 18 Di Martino MT, Gulla A, Cantafo ME, Lionetti M, Leone E, Amodio N *et al*. In vitro and in vivo anti-tumor activity of miR-221/222 inhibitors in multiple myeloma. *Oncotarget* 2013; **4**: 242–255.
- 19 Leone E, Morelli E, Di Martino MT, Amodio N, Foresta U, Gulla A *et al*. Targeting miR-21 inhibits in vitro and in vivo multiple myeloma cell growth. *Clin Cancer Res* 2013; **19**: 2096–2106.
- 20 Amodio N, Di Martino MT, Foresta U, Leone E, Lionetti M, Leotta M *et al*. miR-29b sensitizes multiple myeloma cells to bortezomib-induced apoptosis through the activation of a feedback loop with the transcription factor Sp1. *Cell Death Dis* 2012; **3**: e436.
- 21 Leotta M, Biamonte L, Raimondi L, Ronchetti D, Di Martino MT, Botta C *et al*. A p53-dependent tumor suppressor network is induced by selective miR-125a-5p inhibition in multiple myeloma cells. *J Cell Physiol* 2014; **229**: 2106–2116.
- 22 Zhao JJ, Lin J, Zhu D, Wang X, Brooks D, Chen M *et al*. miR-30-5p functions as a tumor suppressor and novel therapeutic tool by targeting the oncogenic Wnt/beta-catenin/BCL9 pathway. *Cancer Res* 2014; **74**: 1801–1813.
- 23 Misiewicz-Krzeminska I, Sarasquete ME, Quwaider D, Krzeminski P, Ticona FV, Paino T *et al*. Restoration of microRNA-214 expression reduces growth of myeloma cells through positive regulation of P53 and inhibition of DNA replication. *Haematologica* 2013; **98**: 640–648.
- 24 Pichiorri F, Suh SS, Ladetto M, Kuehl M, Palumbo T, Drandi D *et al*. MicroRNAs regulate critical genes associated with multiple myeloma pathogenesis. *Proc Natl Acad Sci USA* 2008; **105**: 12885–12890.
- 25 Pichiorri F, Suh SS, Rocci A, De Luca L, Taccioli C, Santhanam R *et al*. Downregulation of p53-inducible microRNAs 192, 194, and 215 impairs the p53/MDM2 autoregulatory loop in multiple myeloma development. *Cancer Cell* 2010; **18**: 367–381.
- 26 Rossi M, Amodio N, Di Martino MT, Tagliaferri P, Tassone P, Cho WC. MicroRNA and multiple myeloma: from laboratory findings to translational therapeutic approaches. *Curr Pharma Biotechnol* 2014; **15**: 459–467.
- 27 Raimondi L, Amodio N, Di Martino MT, Altomare E, Leotta M, Caracciolo D *et al*. Targeting of multiple myeloma-related angiogenesis by miR-199a-5p mimics: in vitro and in vivo anti-tumor activity. *Oncotarget* 2014; **5**: 3039–3054.
- 28 Scognamiglio I, Di Martino MT, Campani V, Virgilio A, Galeone A, Gulla A *et al*. Transferrin-conjugated SNALPs encapsulating 2'-O-methylated miR-34a for the treatment of multiple myeloma. *BioMed Res Int* 2014; **2014**: 217365.
- 29 Di Martino MT, Campani V, Misso G, Gallo Cantafo ME, Gulla A, Foresta U *et al*. In vivo activity of miR-34a mimics delivered by stable nucleic acid lipid particles (SNALPs) against multiple myeloma. *PLoS One* 2014; **9**: e90005.
- 30 Amodio N, Bellizzi D, Leotta M, Raimondi L, Biamonte L, D'Aquila P *et al*. miR-29b induces SOCS-1 expression by promoter demethylation and negatively regulates migration of multiple myeloma and endothelial cells. *Cell Cycle* 2013; **12**: 3650–3662.
- 31 Lionetti M, Musto P, Di Martino MT, Fabris S, Agnelli L, Todoerti K *et al*. Biological and clinical relevance of miRNA expression signatures in primary plasma cell leukemia. *Clin Cancer Res* 2013; **19**: 3130–3142.
- 32 Rossi M, Pitari MR, Amodio N, Di Martino MT, Conforti F, Leone E *et al*. miR-29b negatively regulates human osteoclastic cell differentiation and function: implications for the treatment of multiple myeloma-related bone disease. *J Cell Physiol* 2013; **228**: 1506–1515.
- 33 Amodio N, Leotta M, Bellizzi D, Di Martino MT, D'Aquila P, Lionetti M *et al*. DNA-demethylating and anti-tumor activity of synthetic miR-29b mimics in multiple myeloma. *Oncotarget* 2012; **3**: 1246–1258.
- 34 Tagliaferri P, Rossi M, Di Martino MT, Amodio N, Leone E, Gulla A *et al*. Promises and challenges of MicroRNA-based treatment of multiple myeloma. *Curr Cancer Drug Targets* 2012; **12**: 838–846.
- 35 Bader AG. miR-34 - a microRNA replacement therapy is headed to the clinic. *Front Genet* 2012; **3**: 120.
- 36 Shirdel EA, Xie W, Mak TW, Jurisica I. NAViGaTing the micronome—using multiple microRNA prediction databases to identify signalling pathway-associated microRNAs. *PLoS One* 2011; **6**: e17429.
- 37 Gururajan M, Haga CL, Das S, Leu CM, Hodson D, Josson S *et al*. MicroRNA 125b inhibition of B cell differentiation in germinal centers. *Int Immunol* 2010; **22**: 583–592.
- 38 Holien T, Vatsveen TK, Hella H, Waage A, Sundan A. Addiction to c-MYC in multiple myeloma. *Blood* 2012; **120**: 2450–2453.
- 39 Chang TC, Yu D, Lee YS, Wentzel EA, Arking DE, West KM *et al*. Widespread microRNA repression by Myc contributes to tumorigenesis. *Nat Genet* 2008; **40**: 43–50.
- 40 Popowski M, Ferguson HA, Sion AM, Koller E, Knudsen E, Van Den Berg CL. Stress and IGF-I differentially control cell fate through mammalian target of rapamycin (mTOR) and retinoblastoma protein (pRb). *J Biol Chem* 2008; **283**: 28265–28273.
- 41 Shi Y, Frost P, Hoang B, Benavides A, Gera J, Lichtenstein A. IL-6-induced enhancement of c-Myc translation in multiple myeloma cells: critical role of cytoplasmic localization of the rna-binding protein hnRNP A1. *J Biol Chem* 2011; **286**: 67–78.
- 42 Li X, Bian Y, Takizawa Y, Hashimoto T, Ikoma T, Tanaka J *et al*. ERK-dependent downregulation of Skp2 reduces Myc activity with HGF, leading to inhibition of cell proliferation through a decrease in Id1 expression. *Mol Cancer Res* 2013; **11**: 1437–1447.
- 43 Delmore JE, Issa GC, Lemieux ME, Rahl PB, Shi J, Jacobs HM *et al*. BET bromodomain inhibition as a therapeutic strategy to target c-Myc. *Cell* 2011; **146**: 904–917.
- 44 Gong J, Zhang JP, Li B, Zeng C, You K, Chen MX *et al*. MicroRNA-125b promotes apoptosis by regulating the expression of Mcl-1, Bcl-w and IL-6R. *Oncogene* 2013; **32**: 3071–3079.
- 45 Shaham L, Binder V, Gefen N, Borkhardt A, Izraeli S. MiR-125 in normal and malignant hematopoiesis. *Leukemia* 2012; **26**: 2011–2018.
- 46 Sun YM, Lin KY, Chen YQ. Diverse functions of miR-125 family in different cell contexts. *J Hematol Oncol* 2013; **6**: 6.
- 47 Kumar M, Lu Z, Takwi AA, Chen W, Callander NS, Ramos KS *et al*. Negative regulation of the tumor suppressor p53 gene by microRNAs. *Oncogene* 2011; **30**: 843–853.
- 48 Murray MY, Rushworth SA, Zaitseva L, Bowles KM, Macewan DJ. Attenuation of dexamethasone-induced cell death in multiple myeloma is mediated by miR-125b expression. *Cell Cycle* 2013; **12**: 2144–2153.
- 49 Chaudhuri AA, So AY, Sinha N, Gibson WS, Taganov KD, O'Connell RM *et al*. MicroRNA-125b potentiates macrophage activation. *J Immunol* 2011; **187**: 5062–5068.
- 50 So AY, Sookram R, Chaudhuri AA, Minisandram A, Cheng D, Xie C *et al*. Dual mechanisms by which miR-125b represses IRF4 to induce myeloid and B-cell leukemias. *Blood* 2014; **124**: 1502–1512.
- 51 Calimeri T, Battista E, Conforti F, Neri P, Di Martino MT, Rossi M *et al*. A unique three-dimensional SCID-polymeric scaffold (SCID-synth-hu) model for in vivo expansion of human primary multiple myeloma cells. *Leukemia* 2011; **25**: 707–711.



This work is licensed under a Creative Commons Attribution-NonCommercial-NoDerivs 4.0 International License. The images or other third party material in this article are included in the article's Creative Commons license, unless indicated otherwise in the credit line; if the material is not included under the Creative Commons license, users will need to obtain permission from the license holder to reproduce the material. To view a copy of this license, visit <http://creativecommons.org/licenses/by-nc-nd/4.0/>

Supplementary Information accompanies this paper on the Leukemia website (<http://www.nature.com/leu>)